KirBac1.1: It's an Inward Rectifying Potassium Channel

Wayland W.L. Cheng,[1] Decha Enkvetchakul,[2] and Colin G. Nichols[1]

[1]Department of Cell Biology and Physiology, Washington University School of Medicine, St. Louis, MO 63110
[2]Department of Pharmacological and Physiological Science, Saint Louis University School of Medicine, St. Louis, MO 63104

KirBac1.1 is a prokaryotic homologue of eukaryotic inward rectifier potassium (Kir) channels. The crystal structure of KirBac1.1 and related KirBac3.1 have now been used extensively to generate in silico models of eukaryotic Kir channels, but functional analysis has been limited to $^{86}Rb^+$ flux experiments and bacteria or yeast complementation screens, and no voltage clamp analysis has been available. We have expressed pure full-length His-tagged KirBac1.1 protein in *Escherichia coli* and obtained voltage clamp recordings of recombinant channel activity in excised membrane patches from giant liposomes. Macroscopic currents of wild-type KirBac1.1 are K^+ selective and spermine insensitive, but blocked by Ba^{2+}, similar to "weakly rectifying" eukaryotic Kir1.1 and Kir6.2 channels. The introduction of a negative charge at a pore-lining residue, I138D, generates high spermine sensitivity, similar to that resulting from the introduction of a negative charge at the equivalent position in Kir1.1 or Kir6.2. KirBac1.1 currents are also inhibited by PIP_2, consistent with $^{86}Rb^+$ flux experiments, and reversibly inhibited by short-chain di-c8-PIP_2. At the single-channel level, KirBac1.1 channels show numerous conductance states with two predominant conductances (15 pS and 32 pS at −100 mV) and marked variability in gating kinetics, similar to the behavior of KcsA in recombinant liposomes. The successful patch clamping of KirBac1.1 confirms that this prokaryotic channel behaves as a bona fide Kir channel and opens the way for combined biochemical, structural, and electrophysiological analysis of a tractable model Kir channel, as has been successfully achieved for the archetypal K^+ channel KcsA.

The Journal of General Physiology

INTRODUCTION

Inward rectifier potassium (Kir) channels are important for regulating excitability in numerous cell types (Nichols and Lopatin, 1997; Ashcroft, 2005; Dhamoon and Jalife, 2005; Flagg and Nichols, 2005; Miki and Seino, 2005; Butt and Kalsi, 2006). Among eukaryotes, they are encoded by the KCNJ gene family. These channels are inward rectifiers in that their conductance increases with hyperpolarization and decreases with depolarization, an effect that results, physiologically, from voltage-dependent block by Mg^{2+} and polyamines (Nichols and Lopatin, 1997). The strength of inward rectification is dependent on the presence of a negatively charged residue in the pore-lining M2 helix called the "rectification controller," amino acid D172 in the strong inward rectifier, Kir2.1 (Lu and MacKinnon, 1994; Stanfield et al., 1994; Wible et al., 1994). Mutation of the rectification controller residue to aspartate in the weakly inward rectifying channels Kir1.1 (N171D) and Kir6.2 (N160D) confers strong sensitivity to polyamine block (Lu and MacKinnon, 1994; Shyng et al., 1997). These Kir channels, particularly Kir2.1 and Kir6.2 (N160D), have served as models to further explore the molecular basis of inward rectification. For example, they have been used to gain insight into the mechanism of steeply voltage-dependent polyamine block (Pearson and Nichols, 1998; Spassova and Lu, 1998; Lu, 2004) and the location of the polyamine binding site (Guo et al., 2003; Guo and Lu, 2003; Kurata et al., 2004, 2006).

Since the discovery of KirBac, a family of prokaryotic genes homologous to eukaryotic Kirs (Durell and Guy, 2001), KirBac1.1, KirBac3.1, and more recently, a KirBac3.1/Kir3.1 chimera, have been crystallized, revealing transmembrane structures that resemble the prototypical potassium channel, KcsA (Kuo et al., 2003, 2005; Nishida et al., 2007). Importantly, these structures also show a large cytoplasmic pore-forming domain and an N-terminal interfacial helix. Attempts to model ligand interactions and molecular dynamics in eukaryotic Kir channels have relied on generating homology models based on the KirBac structures (Antcliff et al., 2005; Haider et al., 2007a,b). Although the predictions of these models are largely consistent with functional data, functional studies of KirBac1.1 itself are essential to make such structural inferences by homology. We have successfully used a liposome $^{86}Rb^+$ uptake assay to demonstrate that KirBac1.1 generates a potassium-selective permeability that can be inhibited by Ba^{2+}, Ca^{2+}, and by acidic conditions (Enkvetchakul et al., 2004).

Correspondence to Colin G. Nichols: cnichols@wustl.edu

Abbreviations used in this paper: Kir, inward rectifier potassium; MTSET, [2-(trimethylammonium)ethyl] methanethiosulfonate; WT, wild-type.

The Rockefeller University Press $30.00
J. Gen. Physiol. Vol. 133 No. 3 295–305
www.jgp.org/cgi/doi/10.1085/jgp.200810125

In contrast to all eukaryotic Kir channels, KirBac1.1 activity is inhibited by phosphatidylinositol phosphates, such as PIP_2 (Enkvetchakul et al., 2005).

Until now, functional studies of KirBac1.1 have been limited to such $^{86}Rb^+$ flux assays of proteoliposomes as well as bacteria or yeast complementation screens (Enkvetchakul et al., 2004; Sun et al., 2006), and no voltage clamp analysis has been reported. Here, we present the first electrophysiological evidence that KirBac1.1 generates functional, potassium-selective channels that exhibit the same key features of rectification found in eukaryotic Kir channels. Wild-type (WT) KirBac1.1 is blocked strongly by barium but only weakly by spermine. However, just as in Kir6.2 (N160D) and Kir1.1 (N171D), mutation of the equivalent pore-lining rectification controller residue in KirBac1.1 to aspartate (I138D) introduces steeply voltage-dependent rectification in spermine. Consistent with $^{86}Rb^+$ flux experiments, KirBac1.1 currents are inhibited by PIP_2. At the single-channel level, WT and mutant KirBac1.1 channels show multiple conductance states and variable open probability and intraburst kinetics. Lastly, we show by voltage clamp recording that R49C, an inactive mutant, can be rescued by [2-(trimethylammonium)ethyl] methanethiosulfonate (MTSET) modification. The results confirm that KirBac1.1 is a bona fide Kir channel in which we now have the unique capability to study using electrophysiology in addition to biochemical and structural techniques.

MATERIALS AND METHODS

Molecular Biology and Protein Purification

The methods used were described previously (Enkvetchakul et al., 2004). In brief, KirBac1.1 was cloned from *Burkholderia pseudomallei* by PCR and subcloned into the pQE60 vector (QIAGEN) with a C-terminal 6-His tag. Mutations were made with the Quikchange Site-Directed Mutagenesis kit (Agilent Technologies) and confirmed by DNA sequencing. For protein purification, BL21* (DE3) cells were transformed with KirBac1.1 in pQE60 and induced with isopropyl β-d-thiogalactopyranoside. The bacteria were lysed by freeze-thaw, solubilized for 2 h in 30 mM decylmaltoside (Anatrace), and centrifuged at 30,000 *g* for 30 min. The supernatant was incubated for 1 h with cobalt beads (~0.2 ml/L bacteria), washed with 40 bed volumes of wash buffer (50 mM Tris-HCl, pH 8.0, 150 mM KCl, 10 mM imidazole, and 5 mM decylmaltoside), and eluted with 1–2 bed volumes of wash buffer with 500 mM imidazole.

$^{86}Rb^+$ Flux Assay

POPE (1-palmitoyl-2-oleoyl-3-phosphatidylethanolamine) and POPG (1-palmitoyl-2-oleoyl-3-phosphatidylglycerol; Avanti Polar Lipids, Inc.) were solubilized in buffer A (450 mM KCl, 10 mM HEPES, and 4 mM NMG, pH 7) with 35 mM CHAPS, mixed at a 3:1 ratio, and incubated at room temperature for 2 h. Polystyrene columns (Thermo Fisher Scientific) were packed with Sephadex G-50 beads, presoaked overnight in buffer A, and spun at 1,500 *g* on a Beckman TJ6 centrifuge (3,000 rpm). For each sample, 6 µg of protein was added to 100 µl of lipid (1 mg) and incubated for 20 min. Liposomes were formed by adding the protein/lipid sample to the partially dehydrated columns and spinning at 1,000 *g*. The extraliposomal solution was exchanged by spinning the sample at 1,000 *g* in partially dehydrated columns, now containing beads soaked in buffer B (450 mM sorbitol, 10 mM HEPES, and 4 mM NMG, pH 7). Uptake was initiated by adding 400 µl buffer C with 1–5 µl $^{86}Rb^+$ and varying concentrations of spermine. At various time points, aliquots were flowed through 0.5-ml Dowex cation exchange columns in the $NMGH^+$ form to remove extraliposomal $^{86}Rb^+$. These aliquots were then mixed with scintillation fluid and counted in a liquid scintillation counter.

Liposome Patch Clamp

POPE and POPG were solubilized in K-MOPS buffer (10 mM MOPS acid, pH 7.4, 158 mM KCl, and 35 mM CHAPS) and mixed at a 3:1 ratio (a total of 4 mg). Purified KirBac1.1 protein was added to the lipids at lipid to protein mass ratios ranging from 200:1 (single-channel recordings) to 20:1 (macroscopic recordings) and

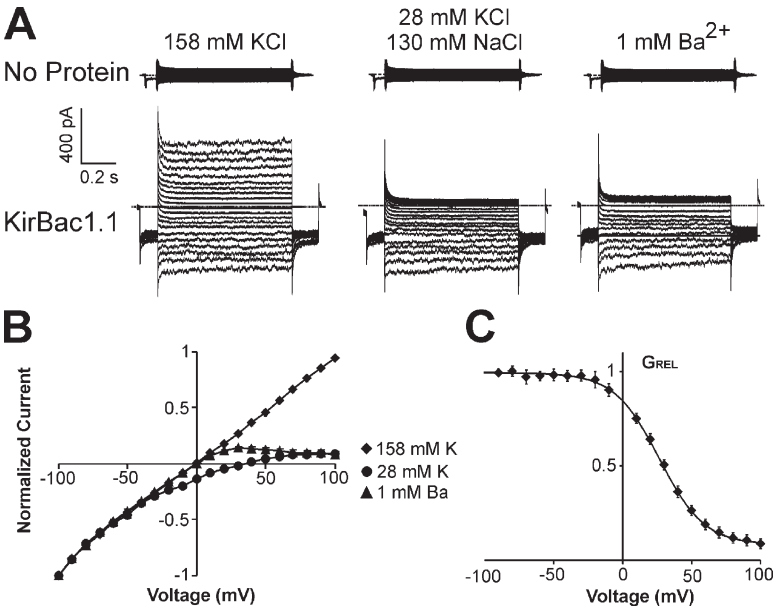

Figure 1. KirBac1.1 voltage-clamped currents are potassium selective and blocked by barium. Inside-out patches were excised from giant liposomes reconstituted with (A) no protein or (B) WT KirBac1.1. (A) Representative currents from an inside-out patch from giant liposomes without KirBac1.1 protein. The pipette was filled with 158 mM K^+ and the bath with the indicated solutions. The voltage was held at −50 mV and then stepped from −100 to +100 mV at 10-mV increments. (B) Representative currents from giant liposomes reconstituted with KirBac1.1 as in A. (C) Plot of normalized current versus voltage for WT KirBac1.1 in the solutions shown in B ($n = 6$ ± SEM). (D) Relative conductance versus voltage plot of KirBac1.1 block in 1 mM Ba^{2+} ($n = 6$ ± SEM). Fitting with a Boltzmann function gives the following parameter values: $V_{1/2} = 25$ mV, $\delta z = 1.5$, residual $G_{REL} = 0.08$, scaling factor = 0.9.

incubated at room temperature for 30 min. Liposomes were formed by detergent removal with Bio-Beads SM-2 Adsorbent (Bio-Rad Laboratories) and centrifuged at 100,000 *g* for 1 h at 4°C (TL-100; Beckman Coulter). The liposome pellet was resuspended in 20 µl K-MOPS buffer and dried in a desiccator as 3–5-µl spots on a clean microscope slide for ~1 h or until completely dried. These spots were then rehydrated with 20 µl K-MOPS buffer overnight at 4°C. Rehydration at room temperature for ~2 h the next day was sufficient to form giant liposomes.

For patch clamping, a glass coverslip was coated overnight with 1 mg/ml polylysine. The giant proteo-liposomes were pipetted onto the polylysine-coated coverslip in an oil-gate chamber (Lederer and Nichols, 1989) and allowed to settle for ~5 min before starting the solution exchange to wash away debris. Unless indicated, patch clamp recordings were performed in symmetrical conditions of K-MOPS buffer. PIP_2 from porcine brain extract and synthetic Di-C8-PIP_2 were purchased from Avanti Polar Lipids, Inc. Membrane patches were voltage clamped using a CV-4 headstage, an Axopatch 1-D amplifier, and a Digidata 1322A digitizer board (MDS Analytical Technologies). Patch pipettes were pulled from soda lime glass microhematocrit tubes (Kimble) to a resistance of ~2–3 MΩ. The voltage step protocol for blocking measurements stepped from −100 to +100 mV at 10-mV increments, holding at −50 mV briefly before each step. Single-channel data were digitized at a sampling rate of 3 kHz, and a low-pass analogue filter was set to 1 kHz. Idealization of single-channel data and generation of amplitude histograms were performed using the pClamp 9.2 software suite (MDS Analytical Technologies). The remaining data analysis was performed using Excel (Microsoft).

RESULTS

Electrical Characterization of KirBac1.1

Excised patch clamp experiments were performed using giant liposomes reconstituted with or without KirBac1.1 in symmetrical, 158-mM KCl except as indicated (Fig. 1 A). Patches from liposomes without protein yielded minimal currents. In contrast, recordings from liposomes reconstituted with KirBac1.1 show significant current with a near linear voltage–current relationship in symmetrical K^+ conditions. When bath K^+ is lowered to 28 mM, there is a +31 ± 1 mV (n = 6; SEM) shift in the reversal potential. The largest shift observed was +34 mV, indicating a minimum K^+/Na^+ permeability ratio of 10:1. Current at positive voltages is blocked by 1 mM Ba^{2+} (Fig. 1 B), with a $V_{1/2}$ of 25 mV and a zδ of 1.5 (Fig. 1 C). The data indicate that these currents are due to functional potassium-selective channels.

We have previously shown by $^{86}Rb^+$ flux experiments that, unlike eukaryotic Kir channels, KirBac1.1 activity is inhibited by PIP_2 (Enkvetchakul et al., 2005). This behavior is recapitulated in voltage clamp recordings (Fig. 2 A) with almost complete channel inhibition by 5 µM PIP_2 (94 ± 3% inhibition; n = 5; SEM). This method of applying micellar PIP_2 to excised membrane patches has been widely used for eukaryotic Kir channels, which are activated by incorporation of PIP_2 in the inner leaflet of the membrane (Fan and Makielski, 1997; Shyng et al., 2000). If micellar PIP_2 incorporates into only one side of the membrane, KirBac1.1 inhibition should be dependent on channel orientation. The fact that PIP_2 inhibits almost all the current in a patch suggests that most KirBac1.1 channels reconstituted in giant liposomes are oriented with their intracellular domain toward the inside of the liposome and exposed to bath solution in inside-out patch (see Discussion). Inhibition by long-chain micellar PIP_2 from porcine brain extract was irreversible during the time scale of the recording (Fig. 2, A and C). However, di-C8-PIP_2, a synthetic water-soluble dioctanoyl form of PIP_2, causes reversible inhibition of KirBac1.1 (Fig. 2, B and C), washing out with a time constant of 27 ± 5 s (n = 3). This is consistent with

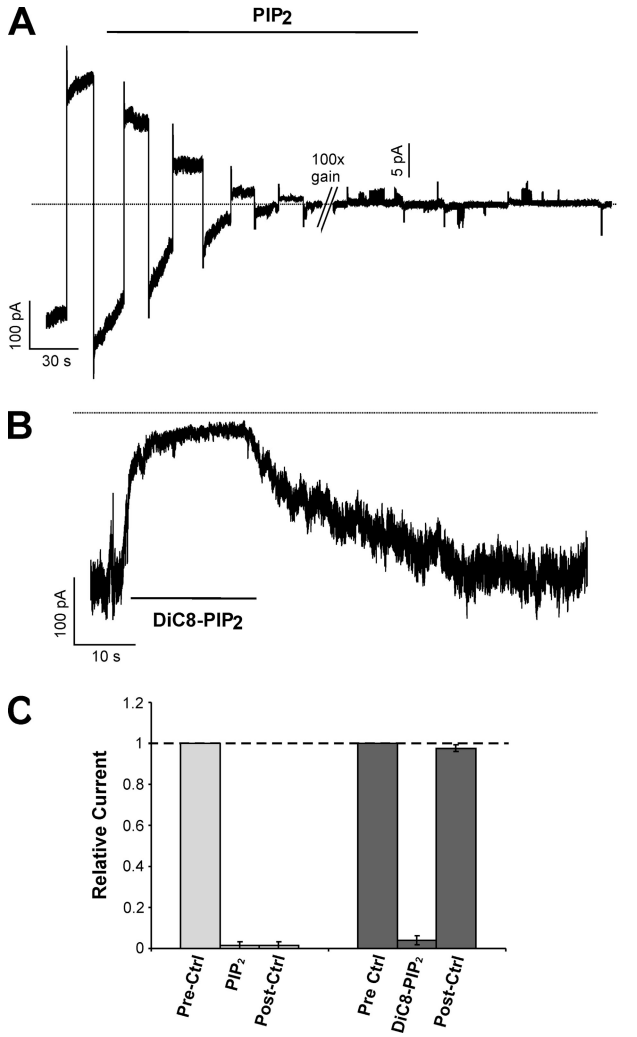

Figure 2. KirBac1.1 currents are inhibited by PIP_2. (A) Continuous recording of potassium-selective and barium-sensitive KirBac1.1 current alternating between +100 and −100 mV clamp. The patch was moved into a 5-µM PIP_2 buffer where indicated. The gain on the amplifier was increased by 100× where indicated. (B) Continuous recording of KirBac1.1 current held at −100 mV. 50 µM diC8-PIP_2 was applied where indicated. (C) Data from recordings for PIP_2 (n = 5) and diC8-PIP_2 (n = 3) inhibition. Currents in PIP_2, diC8-PIP_2, and after 2 min of washout (post-ctrl) are normalized to the initial current (prectrl).

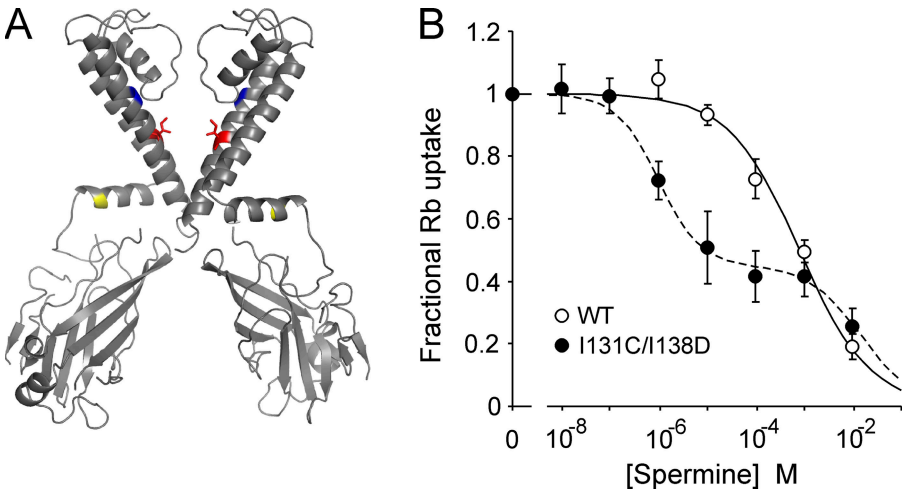

Figure 3. The I131C/I138D mutant is more sensitive to spermine inhibition than WT. (A) Structure of two opposing subunits of KirBac1.1 highlighting the residues I131 (blue) and I138 (red) that were mutated to cysteine and asparate, respectively. R49 is also highlighted in yellow. Mutation of this residue to a cysteine renders an inactive channel that can be rescued by MTSET modification. (B) Plot of relative $^{86}Rb^+$ uptake of WT and I131C/I138D in liposomes at different concentrations of externally applied spermine, normalized to uptake without spermine ($n = 9 \pm$ SEM). The I131C/I138D data are fit with the sum of two Hill functions ($K_{1/2}$ = 1 µM, H = 1; $K_{1/2}$ = 15 mM, H = 0.8), and the WT data with one ($K_{1/2}$ = 0.8 mM, H = 0.6).

previously reported reversible activation of eukaryotic Kir channels by this synthetic short acyl-chain lipid (Rohacs et al., 1999, 2002). This suggests that the dependence of the kinetics of KirBac1.1 inhibition on the hydrocarbon chains of phosphotidylinositol phosphates is similar to that of activation in eukaryotic Kirs, and argues that inhibition and activation occur by a similar mechanism involving partitioning into the membrane and direct interaction with the channel.

Strong Rectification in KirBac1.1 I131C/I138D

WT KirBac1.1 behaves as a weak inward rectifier and is insensitive to block by spermine in both patch clamp and $^{86}Rb^+$ flux assays (Figs. 3 B and 4 A). We hypothesized that mutation of I138, which is equivalent to the rectification controller residue in eukaryotic Kir channels, to an aspartate would confer sensitivity to polyamines just as in Kir1.1 (N171D) and Kir6.2 (N160D; Fig. 3 A, red). However, multiple preparations of I138D mutant KirBac1.1 were inactive when tested by the $^{86}Rb^+$ flux assay (not depicted). We have found that mutation of residue 131 (located in the upper region of TM2, adjacent to the base of the pore helix and near the selectivity filter; Fig. 3 A, blue) from isoleucine to cysteine stabilizes the channel tetramer in SDS-PAGE (Wang et al., 2008). On the I131C background, the I138D mutant generated functional channels assessed by $^{86}Rb^+$ flux (Fig. 3 B). $^{86}Rb^+$ flux assays of WT and I131C/I138D in different concentrations of spermine illustrate that the double mutant, I131C/I138D, is strongly inhibited by spermine, and the concentration dependence of inhibition shows two distinct components. The I131C/I138D data can be fit with the sum of two Hill equations ($K_{1/2}$ = 1 µM and 15 mM), and the WT data with a single Hill equation ($K_{1/2}$ = 0.8 mM). The fact that only 50% of $^{86}Rb^+$ uptake is inhibited with high affinity is consistent with the generation of high affinity block only to internal/cytoplasmic spermine in I131C/I138D, and with channels being bi-directionally oriented (see Discussion).

I131C/I138D also produces K^+-selective and Ba^{2+}-sensitive currents by patch clamp (Fig. 4). WT currents, as well as I131C currents (not depicted), are blocked by 1 mM Ba^{2+} but are essentially insensitive to spermine (Fig. 4 A), whereas I131C/I138D currents are potently blocked by spermine (Fig. 4 B), with steep voltage dependence (for Ba^{2+}, a $V_{1/2}$ of −8 mV and a zδ of 1.2; for spermine, a $V_{1/2}$ of −20 mV and a zδ of 2.5). $V_{1/2}$ varies with blocker concentration and is an indication of blocker affinity, whereas zδ does not change with blocker concentration and is likely a reflection, in part, of the blocker forcing permeant ions across the membrane electric field (Pearson and Nichols, 1998; Spassova and Lu, 1998). It is notable that, in contrast to the ∼50% high affinity spermine inhibition in the liposome flux assay, 80–90% of WT and I131C/I138D currents are consistently blocked with a single voltage-dependent component by Ba^{2+} (WT and I131C/I138D) and spermine (I131C/I138D), which suggests that the channels are not bi-directionally oriented (50:50) in the excised patches from giant liposomes as they are in the smaller liposomes used for the $^{86}Rb^+$ flux assay (see Discussion). I131C/I138D also shows stronger block by 1 mM Ba^{2+} ($V_{1/2}$ = −8 mV) compared with WT ($V_{1/2}$ = 25 mV) or I131C ($V_{1/2}$ = 21 mV), with a partial block of current that appears voltage independent, at least up to −100 mV. In summary, introduction of I138D, the rectification controller position in KirBac1.1, on the I131C background produces functional channels that exhibit steep voltage-dependent block by spermine.

Complex Single-Channel Properties: Multiple Conductances and Gating Heterogeneity

Patch clamp recordings that resolve single-channel openings are readily obtained by reconstituting liposomes with smaller amounts of protein. Fig. 5 shows recordings

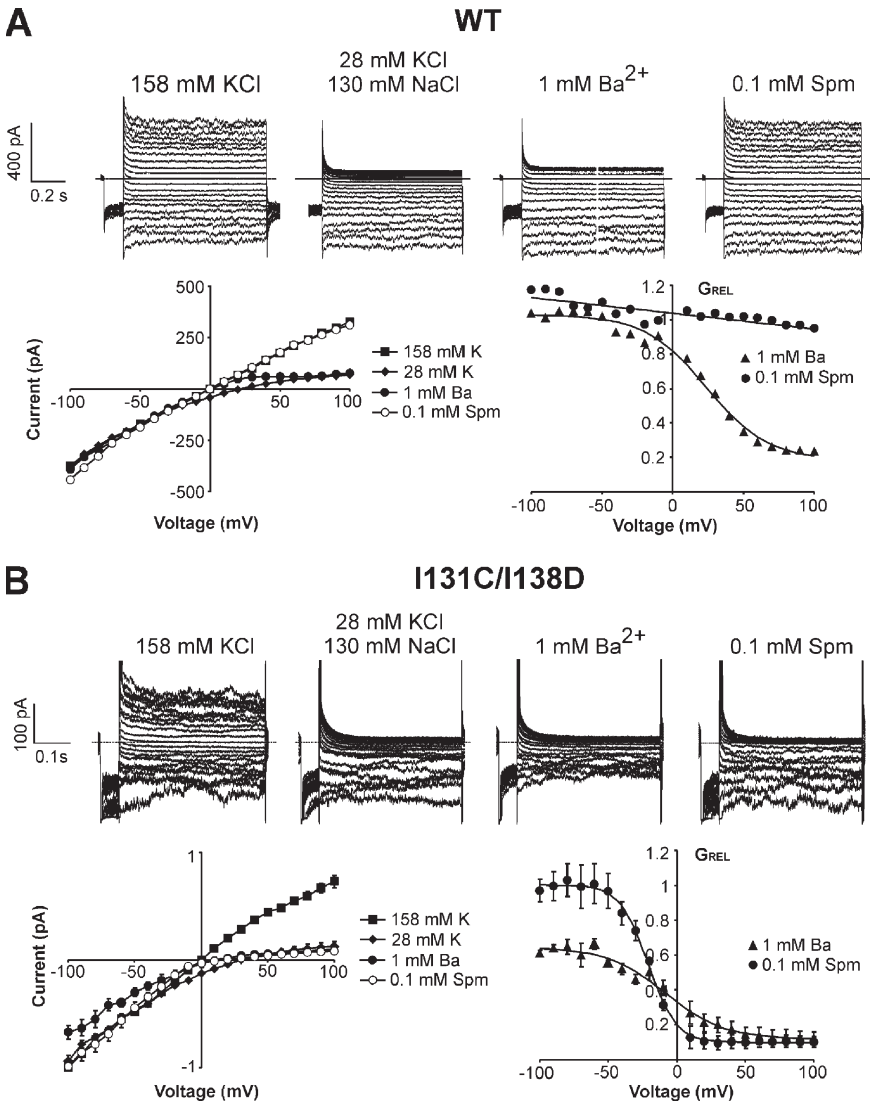

Figure 4. I131C/I138D is blocked by spermine with strong voltage dependence. Voltage step recordings are presented, as in Fig. 1, of (A) WT KirBac1.1 and (B) I131C/I138D in the indicated solutions. (A) Representative recordings of WT KirBac1.1 and its corresponding I-V and G_{REL}-V curves. (B) Representative recordings of I131C/I138D and its corresponding I-V and G_{REL}-V curves (n = 4 ± SEM). The relative conductance curves are fit with Boltzmann functions with the following parameter values: for 1 mM Ba^{2+}: $V_{1/2}$ = −8 mV, δz = 1.2, scaling factor = 0.5, and residual G_{REL} = 0.1; for 0.1 mM spermine: $V_{1/2}$ = −21 mV, δz = 2.5, scaling factor = 0.9, and residual G_{REL} = 0.1.

of WT, I131C/I138D, and I131C with variable numbers of channels in a patch held at +100 mV. At single-channel resolution, WT and I131C activity are blocked by 1 mM Ba^{2+} but insensitive to 0.1 mM spermine, whereas I131C/I138D is potently blocked by spermine, consistent with the macroscopic data.

Single-channel currents of KirBac1.1 also show complex properties, most obviously multiple conductance states. Fig. 6 A shows representative channel openings from two individual patches of WT and I131C/I138D. Both exhibit at least five conductance states. All-points histograms of all channel openings

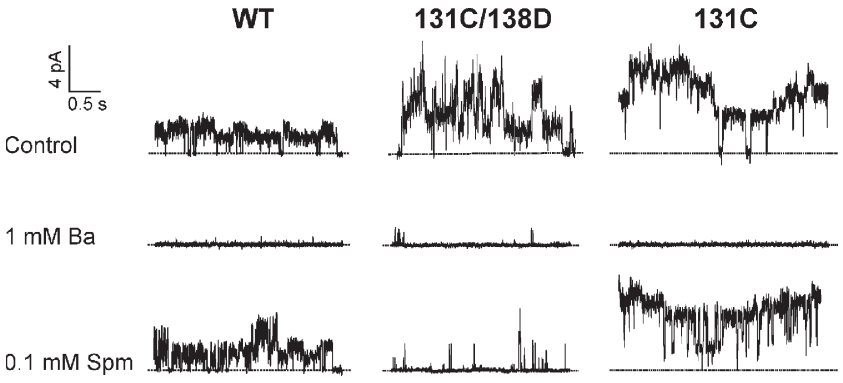

Figure 5. Currents from WT, I131C/I138D, and I131C that resolve single-channel openings are consistent with findings from macroscopic recordings. Shown here are segments from recordings of WT, I131C/I138D, and I131C at +100 mV with the indicated solutions in the bath.

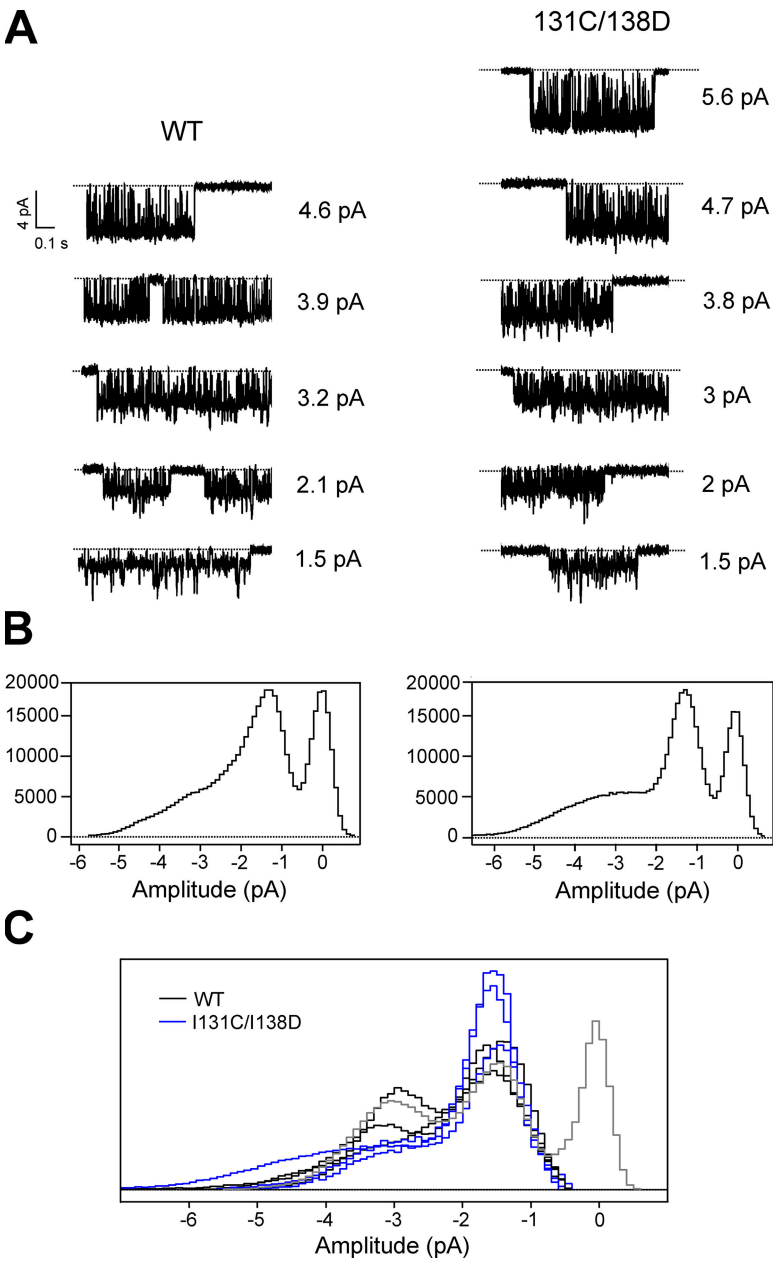

Figure 6. Single-channel openings of KirBac1.1 show multiple conductance levels. (A) The currents shown are representative single-channel openings at −100 mV at all amplitude levels from a patch of WT and I131C/I138D. (B) All-points histograms of all channel openings from each recording. (C) A compilation of all-points histograms of channel openings from WT ($n = 4$; black) and I131C/I138D ($n = 3$; blue) recordings. The baseline (zero-channel current) peak is included for one histogram only (gray), and each histogram is scaled, for the sake of comparison, by dividing the bin values by the total number of points in each respective histogram.

in these two recordings show that smaller conductance states predominate (Fig. 6 B). During bursts of smaller amplitude openings, short transitions to larger conductance states are typically present. The largest single-channel amplitude observed for WT had a conductance of ∼46 pS (chord conductance at −100 mV), and for I131C/I138D, ∼56 pS. However, all single-channel recordings primarily showed two smaller conductance states: the most prevalent at ∼15 pS, and a larger opening at ∼32 pS, measured at −100 mV (Fig. 6 C). These histograms only include channel openings; the area of the baseline peak (Fig. 6 C shows only one in gray) gives no indication of open probability. Fig. 7 A shows all-points histograms of all single-channel openings at +100 and −100 mV from a WT patch, with representative traces from the recording shown above. The red dotted lines in the traces indicate the current levels that correspond with the peaks in the histograms. The two predominant conductance peaks shift to a lower amplitude at +100 mV compared with −100 mV, and stepping from −100 to +100 mV during a single-channel burst shows that the ∼32-pS conductance state at −100 mV corresponds to a conductance of ∼21 pS at +100 mV (Fig. 7 B). All-points histograms were used to determine the major single-channel amplitudes over a range of voltages. Plots of single-channel amplitude versus voltage show that the two major conductance states exhibit a mild intrinsic inward rectification in WT and I131C/I138D (Fig. 7 C; $n = 4$).

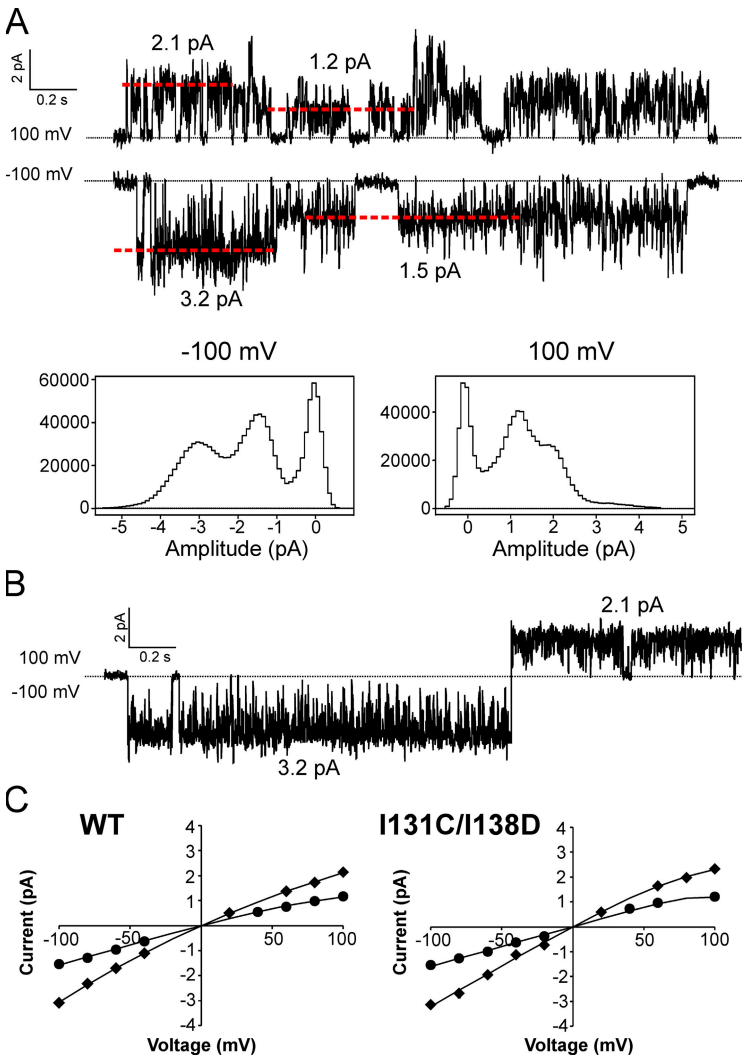

Figure 7. Single-channel amplitudes of KirBac1.1 show two predominant conductance levels and inward rectification. (A) Representative traces from a WT single-channel recording at +100 and −100 mV. The red dashed lines indicate the current amplitudes of the single-channel openings and correspond with the peaks in the histograms. Below are all-points histograms of all channel openings from the entire recording. (B) Single-channel opening from the same recording as in A showing the current amplitude of a single opening/conductance state at −100 and +100 mV. (C) Averaged I-V plots of single-channel amplitudes for WT and I131C/I138D ($n = 4 \pm$ SEM; the error bars are too small to be seen). The data points show only the two most prevalent conductance states (for WT, 15 and 32 pS at −100 mV, 12 and 22 pS at +100 mV). The solid lines have no theoretical meaning.

Single-channel gating kinetics of KirBac1.1 are also complex. Open probability varies significantly from patch to patch. Fig. 8 A shows two WT recordings with contrasting open probabilities. Open probability also tends to be higher at positive voltages than negative voltages, as seen in Fig. 8 B. This may explain why, although WT macroscopic currents show a near linear current–voltage relationship (Fig. 1), single-channel amplitudes exhibit inward rectification (Fig. 7 C). Detailed inspection of these recordings reveals variations in intraburst gating kinetics at negative voltages (Fig. 8 C). Single-channel bursts at −100 mV were individually idealized using a "50% threshold" criterion based on their respective amplitudes determined from all-point histograms (red dashed lines in Fig. 8 C), and the idealized data were used to calculate intraburst open probability. A plot of the intraburst open probability for all bursts in patches of WT and I131C/I138D show at least two gating modes at −100 mV. Generally, most openings have a high P (o) of ∼0.9, but occasionally, openings will switch to a flicker mode where P (o) is ∼0.65. Such gating heterogeneities are uncommon among eukaryotic potassium channels in cellular membranes, but similar behaviors have been reported for KcsA reconstituted in liposomes (Chakrapani et al., 2007b).

One-sided Activation of R49C

In a prior study, using the $^{86}Rb^{+}$ flux assay, we showed that cysteine mutants of KirBac1.1 in the slide helix can be activated by modification with MTS reagents. In particular, the mutations R49C or K57C render the channel inactive, but can be rescued by MTSEA or MTSET modification (Enkvetchakul et al., 2007). KirBac1.1 channels reconstituted in giant liposomes are not necessarily oriented in the same direction as eukaryotic channels expressed in cell membranes. Because R49 is located in the slide helix (Fig. 3 A, yellow), application of MTSET in the bath can only activate those channels in which the "cytoplasmic" end is also facing the bath. Fig. 9 shows a continuous recording of R49C single-channel activity after activation by MTSET. The currents behave exactly as WT: they are inhibited by 1 mM Ba^{2+} but insensitive to 0.1 mM spermine. Amplitude histograms as well as the

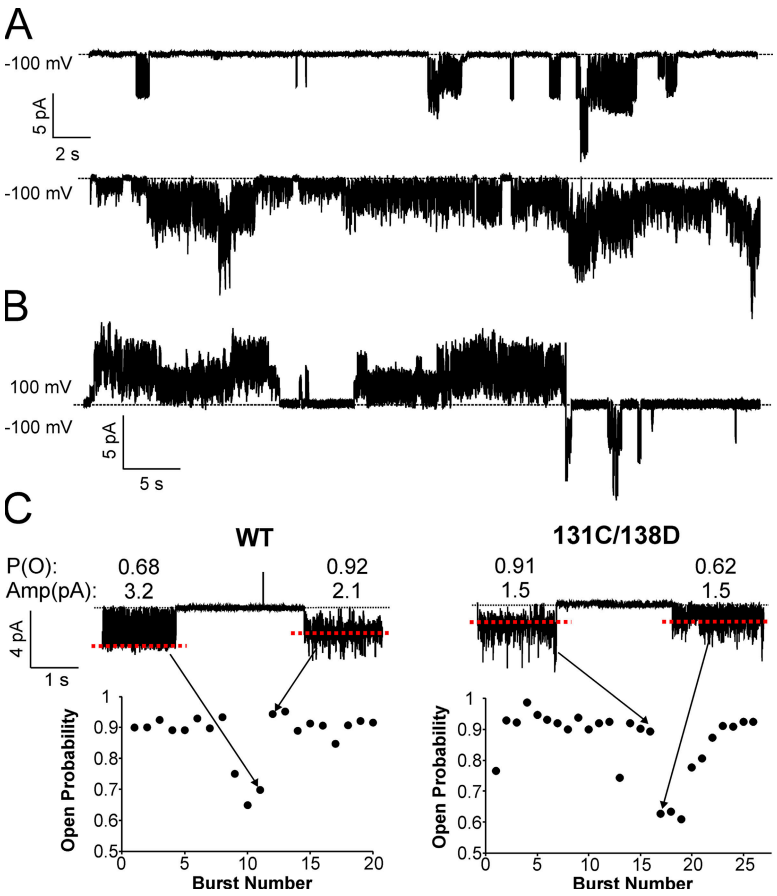

Figure 8. Single-channel recordings show significant gating heterogeneity. (A) Two continuous recordings of WT single channels at −100 mV showing low open probability (top) and high open probability (bottom) currents. (B) A continuous recording of WT single channels at the indicated voltages. (C) Plots of intraburst open probability for every channel burst in a patch of WT and I131C/I138D. The currents above show two bursts at −100 mV with contrasting open probabilities that correspond to the data points indicated by the arrows. Open probability and current amplitude are shown above each burst.

general appearance of channel gating at +100 mV compared with −100 mV are similar to WT and I131C/I138D (Figs. 7, 8, and 9). The fact that WT and I131C/I138D exhibit similar single-channel amplitudes and gating behavior as activated R49C is consistent with most of the reconstituted channels being oriented with their cytoplasmic end facing the bath in an inside-out patch.

DISCUSSION

Validation of KirBac1.1 as a Kir Channel

The prokaryotic potassium channel, KcsA, has been widely used as a model channel to investigate mechanisms of ion permeation, selectivity, and gating. Other prokaryotic potassium channels, such as MthK and KvAP, have followed suit in becoming the subject of numerous structural and electrophysiological studies. Since the structure was solved, however, functional studies of KirBac1.1 have been limited to $^{86}Rb^{+}$ flux assays and bacteria or yeast complementation screens (Enkvetchakul et al., 2004, 2005, 2007; Sun et al., 2006). Here, we demonstrate by patch clamping giant liposomes that KirBac1.1 is a functional potassium channel and that the mutation I138D, equivalent to the rectification controller residue in eukaryotic Kir channels, confers the signature strong inward rectification as in Kir1.1 and Kir6.2. These findings confirm that KirBac1.1 is a bona fide Kir channel and strengthen the validity of structural homology models of eukaryotic Kirs generated using the KirBac1.1 structure. Such homology models will be useful in understanding interactions of polyamines and other blockers within the pore of Kirs.

Multiple Single-Channel Conductances in KirBac1.1

Single-channel analyses of KcsA have revealed unusual features, such as prominent subconductance states and variable gating kinetics, which are rarely seen among eukaryotic channels (Schrempf et al., 1995; Cuello et al., 1998; Meuser et al., 1999; Splitt et al., 2000; Cordero-Morales et al., 2006; Molina et al., 2006; Chakrapani et al., 2007b). Interestingly, we show in this study that KirBac1.1 exhibits many of the same features seen in KcsA, which leads us to speculate whether these differences are attributed to the protein and lipid environment of these prokaryotic channels reconstituted in liposomes compared with that of eukaryotic channels expressed in cell membranes. Indeed, pioneering electrophysiological data for KcsA showed significant differences in channel function, such as single-channel subconductances, between KcsA in giant liposome-protoplast vesicles

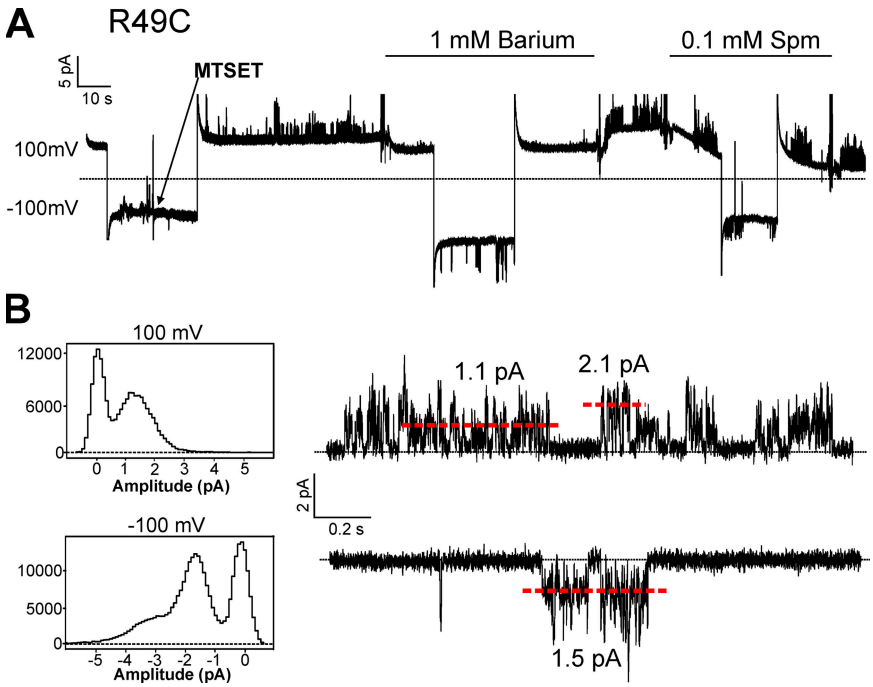

Figure 9. Continuous recording of R49C held at +100 and −100 mV. 0.1 mM MTSET solution was applied as shown by the arrow, and solution changes were made at the indicated bars. Below are all-points histograms of the recording above with representative traces at +100 and −100 mV. The red dashed lines indicate current amplitudes that correspond with peaks in the histograms.

from *Streptomyces lividans* and purified KcsA reconstituted in lipid bilayers (Schrempf et al., 1995).

Several studies have reported multi-conductance behavior in steady-state single-channel recordings of other K^+ channels. For example, Kir2.1 single-channel currents can show multiple levels due to block by micromolar concentrations of cations like Ca^{2+} and Mg^{2+} (Mazzanti et al., 1996; Oishi et al., 1998). Such behavior is unlikely to underlie multiple conductances in the present case because the addition of 1 mM EDTA to the recording solutions does not alter the multi-conductance behavior of KirBac1.1 (not depicted). In KcsA, multiple current levels have been attributed to coupled gating from clusters of channels (Molina et al., 2006). Although the current levels from Fig. 6 are not all obvious multiples of a unit conductance, some are approximately multiples of 1.5 (1.5, 3.2, and 4.6 pA in WT), such that we cannot rule out this possibility.

The multi-conductance behavior of KirBac1.1 could also result from permeant ion interactions with the pore. Studies of single-channel properties of Kir2.1, with mutations in the selectivity filter or in the presence of permeant ions other than K^+, reveal complex subconductance behaviors similar to those observed in this study (Lu et al., 2001a,b). One interesting possibility arises from a series of studies where protonatable residues such as lysine, arginine, and histidine were systematically engineered along the M1 and M2 transmembrane helices of the nicotinic acetylcholine receptor, resulting in two fluctuating conductance levels that correspond to the protonated and deprotonated states (Cymes et al., 2005; Cymes and Grosman, 2008). A similar mechanism, where positively charged moieties in the pore cause subconductances, has been reported in the Kir channel, Kir6.2 (Loussouarn et al., 2001). It is possible that the rapid transitions to and from larger openings observed in the single-channel currents of KirBac1.1 are due, in part, to protonatable residues such as H117, H124, H210, and H219 that produce reversible positive charges near the channel pore.

Orientation of KirBac1.1 Reconstituted in Giant Liposomes

The first electrophysiological studies of KcsA were performed using planar lipid bilayers, and it was quickly recognized that channels could conceivably insert in either orientation (Cuello et al., 1998; Heginbotham et al., 1999; LeMasurier et al., 2001). These studies demonstrated that KcsA is oriented predominantly in one direction in a reconstituted lipid bilayer, which corresponds to the C terminus of the channel facing the bath in an excised patch (Chakrapani et al., 2007a). Several observations from the present study suggest that KirBac1.1 reconstituted in giant liposomes has a similar preference for this orientation. First, Ba^{2+} and spermine block consistently show a single component, leaving ~10% residual current, some of which could be accounted for by leak (Fig. 4). If channel orientation were 50:50, one would expect to see half the current blocked with one affinity and half with another because the binding sites for intracellular and extracellular spermine are predicted to be different. This, in fact, is what is seen with spermine inhibition in the smaller proteoliposomes using the Rb^+ flux assay (Fig. 3 B). The data in Fig. 3 B can also be explained by the presence of two channel conformations with differing affinities for spermine. However, the monophasic and near-complete block by spermine in I131C/I138D observed by patch clamp

rules out biphasic block under these conditions and is instead consistent with: (1) the I138D mutation generating a single high affinity intracellular spermine binding site and (2) most of the channels oriented with their "intracellular" end facing the bath in the excised patch configuration. Intuitively, this difference in channel orientation between the smaller liposomes used for the $^{86}Rb^+$ flux assay and giant liposomes used for patch clamp seems possible because the formation of giant liposomes involves an extra dehydration/rehydration step that could alter orientation (see Materials and methods).

A second observation is that PIP_2 applied in the bath inhibits most KirBac1.1 currents (Fig. 2). Overwhelming evidence from eukaryotic Kir channels indicate that PIP_2 activation occurs by interaction with the cytoplasmic end of the channel at the inner leaflet of the membrane (Fan and Makielski, 1997; Shyng et al., 2000; Cukras et al., 2002; Haider et al., 2007b). PIP_2 inhibition of KirBac1.1 also has a similar dependence on the number of phosphate groups (greater inhibition with more negative charges in the head group) and the length of the lipid tail (short-chain PIP_2 inhibition is reversible), as eukaryotic Kirs (Enkvetchakul et al., 2005). Assuming a similar interaction of PIP_2 with KirBac1.1 as with eukaryotic Kirs, and assuming that PIP_2 partitions into only one side of the membrane leaflet, most of the channels, again, must be oriented with their intracellular end facing the bath. Similar to the spermine block results, extraliposomal application of PIP_2 in the $^{86}Rb^+$ flux assay causes only ~50% inhibition, suggesting a 50:50 orientation in these smaller liposomes (Enkvetchakul et al., 2005).

Lastly, all single-channel recordings consistently show the same amplitude–voltage relationship (inward rectification) and gating pattern, suggesting a preferential channel orientation. Indeed, single-channel currents of MTSET-activated R49C, which requires that the channels be oriented with their cytoplasmic end facing the bath, resemble those of WT and I131C/I138D (Fig. 9). Future electrophysiological studies of KirBac1.1 should focus on resolving this uncertainty about channel sidedness. Cysteine mutants such as R49C and K57C that require MTSET modification for activity should provide a useful tool for isolating channels of a single orientation.

Conclusion

The KirBac1.1 and KirBac3.1 crystal structures have been used extensively in several molecular modeling studies (Grottesi et al., 2005; Domene et al., 2006, 2008; Hellgren et al., 2006; Vemparala et al., 2008). Until now, no electrophysiological data has been available to supplement these computational studies. We report voltage clamp recordings of KirBac1.1 currents and confirm that this prokaryotic protein behaves functionally as a Kir channel. Recent studies of KcsA have been a testament to the power of combining structural and biochemical information with electrophysiology in understanding channel function (Cordero-Morales et al., 2006; Ader et al., 2008). It is now possible to take a similar approach in a model Kir channel and to develop more detailed molecular models of permeation, gating, and strong inward rectification.

We are very grateful to Drs. Paul Schlesinger (Washington University) and Chris Miller (Brandeis University) for their help in our abortive early efforts to detect KirBac1.1 channel activity in planar lipid bilayers.

The work was supported by National Institutes of Health grants HL54171 (to C.G. Nichols) and DK069424 (D. Enkvetchakul).

Lawrence G. Palmer served as editor.

Submitted: 25 September 2008
Accepted: 14 January 2009

REFERENCES

Ader, C., R. Schneider, S. Hornig, P. Velisetty, E.M. Wilson, A. Lange, K. Giller, I. Ohmert, M.F. Martin-Eauclaire, D. Trauner, et al. 2008. A structural link between inactivation and block of a K+ channel. *Nat. Struct. Mol. Biol.* 15:605–612.

Antcliff, J.F., S. Haider, P. Proks, M.S. Sansom, and F.M. Ashcroft. 2005. Functional analysis of a structural model of the ATP-binding site of the KATP channel Kir6.2 subunit. *EMBO J.* 24:229–239.

Ashcroft, F.M. 2005. ATP-sensitive potassium channelopathies: focus on insulin secretion. *J. Clin. Invest.* 115:2047–2058.

Butt, A.M., and A. Kalsi. 2006. Inwardly rectifying potassium channels (Kir) in central nervous system glia: a special role for Kir4.1 in glial functions. *J. Cell. Mol. Med.* 10:33–44.

Chakrapani, S., J.F. Cordero-Morales, and E. Perozo. 2007a. A quantitative description of KcsA gating I: macroscopic currents. *J. Gen. Physiol.* 130:465–478.

Chakrapani, S., J.F. Cordero-Morales, and E. Perozo. 2007b. A quantitative description of KcsA gating II: single-channel currents. *J. Gen. Physiol.* 130:479–496.

Cordero-Morales, J.F., L.G. Cuello, Y.X. Zhao, V. Jogini, D.M. Cortes, B. Roux, and E. Perozo. 2006. Molecular determinants of gating at the potassium-channel selectivity filter. *Nat. Struct. Mol. Biol.* 13:311–318.

Cuello, L.G., J.G. Romero, D.M. Cortes, and E. Perozo. 1998. pH-dependent gating in the Streptomyces lividans K+ channel. *Biochemistry.* 37:3229–3236.

Cukras, C.A., I. Jeliazkova, and C.G. Nichols. 2002. Structural and functional determinants of conserved lipid interaction domains of inward rectifying Kir6.2 channels. *J. Gen. Physiol.* 119:581–591.

Cymes, G.D., and C. Grosman. 2008. Pore-opening mechanism of the nicotinic acetylcholine receptor evinced by proton transfer. *Nat. Struct. Mol. Biol.* 15:389–396.

Cymes, G.D., Y. Ni, and C. Grosman. 2005. Probing ion-channel pores one proton at a time. *Nature.* 438:975–980.

Dhamoon, A.S., and J. Jalife. 2005. The inward rectifier current (IK1) controls cardiac excitability and is involved in arrhythmogenesis. *Heart Rhythm.* 2:316–324.

Domene, C., S. Vemparala, M.L. Klein, C. Venien-Bryan, and D.A. Doyle. 2006. Role of aromatic localization in the gating process of a potassium channel. *Biophys. J.* 90:L01–L03.

Domene, C., S. Vemparala, S. Furini, K. Sharp, and M.L. Klein. 2008. The role of conformation in ion permeation in a K+ channel. *J. Am. Chem. Soc.* 130:3389–3398.

Durell, S.R., and H.R. Guy. 2001. A family of putative Kir potassium channels in prokaryotes. *BMC Evol. Biol.* 1:14.

Enkvetchakul, D., J. Bhattacharyya, I. Jeliazkova, D.K. Groesbeck, C.A. Cukras, and C.G. Nichols. 2004. Functional characterization of a prokaryotic Kir channel. *J. Biol. Chem.* 279:47076–47080.

Enkvetchakul, D., I. Jeliazkova, and C.G. Nichols. 2005. Direct modulation of Kir channel gating by membrane phosphatidylinositol 4,5-bisphosphate. *J. Biol. Chem.* 280:35785–35788.

Enkvetchakul, D., I. Jeliazkova, J. Bhattacharyya, and C.G. Nichols. 2007. Control of inward rectifier K channel activity by lipid tethering of cytoplasmic domains. *J. Gen. Physiol.* 130:329–334.

Fan, Z., and J.C. Makielski. 1997. Anionic phospholipids activate ATP-sensitive potassium channels. *J. Biol. Chem.* 272:5388–5395.

Flagg, T.P., and C.G. Nichols. 2005. Sarcolemmal K(ATP) channels: what do we really know? *J. Mol. Cell. Cardiol.* 39:61–70.

Grottesi, A., C. Domene, B. Hall, and M.S. Sansom. 2005. Conformational dynamics of M2 helices in KirBac channels: helix flexibility in relation to gating via molecular dynamics simulations. *Biochemistry.* 44:14586–14594.

Guo, D., and Z. Lu. 2003. Interaction mechanisms between polyamines and IRK1 inward rectifier K^+ channels. *J. Gen. Physiol.* 122:485–500.

Guo, D., Y. Ramu, A.M. Klem, and Z. Lu. 2003. Mechanism of rectification in inward-rectifier K^+ channels. *J. Gen. Physiol.* 121:261–275.

Haider, S., S. Khalid, S.J. Tucker, F.M. Ashcroft, and M.S. Sansom. 2007a. Molecular dynamics simulations of inwardly rectifying (Kir) potassium channels: a comparative study. *Biochemistry.* 46:3643–3652.

Haider, S., A.I. Tarasov, T.J. Craig, M.S. Sansom, and F.M. Ashcroft. 2007b. Identification of the PIP2-binding site on Kir6.2 by molecular modelling and functional analysis. *EMBO J.* 26:3749–3759.

Heginbotham, L., M. LeMasurier, L. Kolmakova-Partensky, and C. Miller. 1999. Single streptomyces lividans K^+ channels: functional asymmetries and sidedness of proton activation. *J. Gen. Physiol.* 114:551–560.

Hellgren, M., L. Sandberg, and O. Edholm. 2006. A comparison between two prokaryotic potassium channels (KirBac1.1 and KcsA) in a molecular dynamics (MD) simulation study. *Biophys. Chem.* 120:1–9.

Kuo, A., J.M. Gulbis, J.F. Antcliff, T. Rahman, E.D. Lowe, J. Zimmer, J. Cuthbertson, F.M. Ashcroft, T. Ezaki, and D.A. Doyle. 2003. Crystal structure of the potassium channel KirBac1.1 in the closed state. *Science.* 300:1922–1926.

Kuo, A., C. Domene, L.N. Johnson, D.A. Doyle, and C. Venien-Bryan. 2005. Two different conformational states of the KirBac3.1 potassium channel revealed by electron crystallography. *Structure.* 13:1463–1472.

Kurata, H.T., L.R. Phillips, T. Rose, G. Loussouarn, S. Herlitze, H. Fritzenschaft, D. Enkvetchakul, C.G. Nichols, and T. Baukrowitz. 2004. Molecular basis of inward rectification: polyamine interaction sites located by combined channel and ligand mutagenesis. *J. Gen. Physiol.* 124:541–554.

Kurata, H.T., L.J. Marton, and C.G. Nichols. 2006. The polyamine binding site in inward rectifier K^+ channels. *J. Gen. Physiol.* 127:467–480.

Lederer, W.J., and C.G. Nichols. 1989. Nucleotide modulation of the activity of rat heart ATP-sensitive K+ channels in isolated membrane patches. *J. Physiol.* 419:193–211.

LeMasurier, M., L. Heginbotham, and C. Miller. 2001. KcsA: it's a potassium channel. *J. Gen. Physiol.* 118:303–314.

Loussouarn, G., L.R. Phillips, R. Masia, T. Rose, and C.G. Nichols. 2001. Flexibility of the Kir6.2 inward rectifier K(+) channel pore. *Proc. Natl. Acad. Sci. USA.* 98:4227–4232.

Lu, T., A.Y. Ting, J. Mainland, L.Y. Jan, P.G. Schultz, and J. Yang. 2001a. Probing ion permeation and gating in a K+ channel with backbone mutations in the selectivity filter. *Nat. Neurosci.* 4:239–246.

Lu, T., L. Wu, J. Xiao, and J. Yang. 2001b. Permeant ion-dependent changes in gating of Kir2.1 inward rectifier potassium channels. *J. Gen. Physiol.* 118:509–522.

Lu, Z. 2004. Mechanism of rectification in inward-rectifier K+ channels. *Annu. Rev. Physiol.* 66:103–129.

Lu, Z., and R. MacKinnon. 1994. Electrostatic tuning of Mg2+ affinity in an inward-rectifier K+ channel. *Nature.* 371:243–246.

Mazzanti, M., R. Assandri, A. Ferroni, and D. DiFrancesco. 1996. Cytoskeletal control of rectification and expression of four substates in cardiac inward rectifier K+ channels. *FASEB J.* 10:357–361.

Meuser, D., H. Splitt, R. Wagner, and H. Schrempf. 1999. Exploring the open pore of the potassium channel from Streptomyces lividans. *FEBS Lett.* 462:447–452.

Miki, T., and S. Seino. 2005. Roles of KATP channels as metabolic sensors in acute metabolic changes. *J. Mol. Cell. Cardiol.* 38:917–925.

Molina, M.L., F.N. Barrera, A.M. Fernandez, J.A. Poveda, M.L. Renart, J.A. Encinar, G. Riquelme, and J.M. Gonzalez-Ros. 2006. Clustering and coupled gating modulate the activity in KcsA, a potassium channel model. *J. Biol. Chem.* 281:18837–18848.

Nichols, C.G., and A.N. Lopatin. 1997. Inward rectifier potassium channels. *Annu. Rev. Physiol.* 59:171–191.

Nishida, M., M. Cadene, B.T. Chait, and R. MacKinnon. 2007. Crystal structure of a Kir3.1-prokaryotic Kir channel chimera. *EMBO J.* 26:4005–4015.

Oishi, K., K. Omori, H. Ohyama, K. Shingu, and H. Matsuda. 1998. Neutralization of aspartate residues in the murine inwardly rectifying K+ channel IRK1 affects the substate behaviour in Mg2+ block. *J. Physiol.* 510:675–683.

Pearson, W.L., and C.G. Nichols. 1998. Block of the Kir2.1 channel pore by alkylamine analogues of endogenous polyamines. *J. Gen. Physiol.* 112:351–363.

Rohacs, T., J. Chen, G.D. Prestwich, and D.E. Logothetis. 1999. Distinct specificities of inwardly rectifying K(+) channels for phosphoinositides. *J. Biol. Chem.* 274:36065–36072.

Rohacs, T., C. Lopes, T. Mirshahi, T. Jin, H. Zhang, and D.E. Logothetis. 2002. Assaying phosphatidylinositol bisphosphate regulation of potassium channels. *Methods Enzymol.* 345:71–92.

Schrempf, H., O. Schmidt, R. Kummerlen, S. Hinnah, D. Muller, M. Betzler, T. Steinkamp, and R. Wagner. 1995. A prokaryotic potassium ion channel with two predicted transmembrane segments from Streptomyces lividans. *EMBO J.* 14:5170–5178.

Shyng, S., T. Ferrigni, and C.G. Nichols. 1997. Control of rectification and gating of cloned KATP channels by the Kir6.2 subunit. *J. Gen. Physiol.* 110:141–153.

Shyng, S.L., C.A. Cukras, J. Harwood, and C.G. Nichols. 2000. Structural determinants of PIP_2 regulation of inward rectifier K_{ATP} channels. *J. Gen. Physiol.* 116:599–608.

Spassova, M., and Z. Lu. 1998. Coupled ion movement underlies rectification in an inward-rectifier K^+ channel. *J. Gen. Physiol.* 112:211–221.

Splitt, H., D. Meuser, I. Borovok, M. Betzler, and H. Schrempf. 2000. Pore mutations affecting tetrameric assembly and functioning of the potassium channel KcsA from Streptomyces lividans. *FEBS Lett.* 472:83–87.

Stanfield, P.R., N.W. Davies, P.A. Shelton, M.J. Sutcliffe, I.A. Khan, W.J. Brammar, and E.C. Conley. 1994. A single aspartate residue is involved in both intrinsic gating and blockage by Mg2+ of the inward rectifier, IRK1. *J. Physiol.* 478:1–6.

Sun, S., J.H. Gan, J.J. Paynter, and S.J. Tucker. 2006. Cloning and functional characterization of a superfamily of microbial inwardly rectifying potassium channels. *Physiol. Genomics.* 26:1–7.

Vemparala, S., C. Domene, and M.L. Klein. 2008. Interaction of anesthetics with open and closed conformations of a potassium channel studied via molecular dynamics and normal mode analysis. *Biophys. J.* 94:4260–4269.

Wang, S., Y. Alimi, A. Tong, C.G. Nichols, and D. Enkvetchakul. 2008. Differential roles of blocking ions on KirBac1.1 tetramer stability. *J. Biol. Chem.* In press.

Wible, B.A., M. Taglialatela, E. Ficker, and A.M. Brown. 1994. Gating of inwardly rectifying K+ channels localized to a single negatively charged residue. *Nature.* 371:246–249.